J Mol Med (2012) 90:945–957
DOI 10.1007/s00109-012-0860-9

ORIGINAL ARTICLE

Developmental regulation of inflammatory cytokine-mediated Stat3 signaling: the missing link between intrauterine growth restriction and pulmonary dysfunction?

Miguel Angel Alejandre Alcazar · Iris Östreicher · Sarah Appel · Eva Rother · Christina Vohlen · Christian Plank · Jörg Dötsch

Received: 27 September 2011 / Revised: 5 December 2011 / Accepted: 28 December 2011 / Published online: 21 January 2012

Abstract Intrauterine growth restriction (IUGR) is a risk factor for impairment of lung function in adolescence and adulthood. Inflammatory and proliferative processes linking IUGR and perturbed extracellular matrix (ECM) as an underlying mechanism have not been addressed so far. Therefore, in this study, we aimed to investigate the developmental regulation of inflammatory and profibrotic processes in the lung subsequent to IUGR. IUGR was induced in rats by isocaloric protein restriction during gestation. Lung function was assessed with direct plethysmography at postnatal day (P) 28 and P70. Lungs were obtained at P1, P42, and P70 for assessment of mRNA, protein expression, immunohistochemistry, and gelatinolytic activity. Both respiratory system resistance and compliance were impaired subsequent to IUGR at P28 and this impairment was even more pronounced at P70. In line with these results, the expression of ECM components and metabolizing enzymes was deregulated. The deposition of collagen was increased at P70. In addition, the expression of inflammatory cytokines and both the activity and the expression of target genes of Stat3 signaling were dynamically regulated, with unaltered or decreased expression at P1 and significantly increased expression art P70. Taken together, these data give evidence for an age-dependent impairment of lung function as a result of a developmentally regulated increase in inflammatory and profibrotic processes subsequent to IUGR.

Keywords Intrauterine growth restriction · Lung disease · Inflammation · Stat3 · Airway inflammation · Airway hyperresponsiveness

M. A. Alejandre Alcazar (✉) · S. Appel · E. Rother · C. Vohlen · J. Dötsch
Department of Pediatrics and Adolescent Medicine,
University of Cologne,
Kerpener Strasse 62,
50937 Cologne, Germany
e-mail: miguel.alejandre-alcazar@uk-koeln.de

I. Östreicher
Department of Neonatology, Charité University Medical Center,
Berlin, Germany

C. Plank
Department of Pediatrics and Adolescent Medicine,
University of Erlangen—Nuremberg,
Nuremberg, Germany

Introduction

The incidence of respiratory illness has increased during the past several decades in many parts of the world [1]. Bronchial asthma is the most common chronic childhood disease in developed countries. Its prevalence has nearly doubled over the last 2 decades, putting a serious socio-economic burden on the children and their families [2]. The pathogenesis of bronchial asthma is based on the interaction between multiple genetic and environmental factors [3]. Prenatal and postnatal influences, such as maternal smoking during gestation and recurrent respiratory tract infections during infancy can adversely affect later respiratory health [4].

Barker et al. coined the term *intrauterine programming* to reflect that a temporal change in the fetal environment such as intrauterine growth restriction (IUGR) leads to a permanent change of physiological processes later in life [5, 6]. Intrauterine growth restriction affects approximately 10% of all newborns and is a major risk factor for the development

of metabolic syndrome in adulthood [5]. Furthermore, there is an increasing body of evidence that IUGR induces changes in the developing lung with a persisting impairment of pulmonary structure and function [7–9]. In addition, recent epidemiological studies have demonstrated impaired lung function with reduced forced expiratory volume (FEV_1) in young infants following IUGR [10].

However, the molecular pathomechanisms of IUGR-associated lung disease have not been completely clarified so far. Several studies indicate that a severely perturbed extracellular matrix (ECM) metabolism contributes to the impairment of lung function and suggest a regulatory effect of IUGR on the pulmonary structure and production of ECM components [9, 11]. Both lung structure and function are already determined during early and late lung development [12, 13]. Interference with the developmental program of the lung during any of these phases may render the lung less effective in gas exchange and more susceptible to disease. Several experimental studies have demonstrated morphologic pulmonary alterations and imbalance of ECM composition in lungs of animals subsequent to IUGR [7, 8]. Additionally, analysis of lung structure in intrauterine growth restricted animals revealed an impaired development of the lung. For example, maturation of the surfactant system is controversially discussed: there are studies reporting a delayed maturation of the surfactant proteins subsequent to IUGR [14], whereas other groups either state no alterations [15, 16] or increased maturation of the surfactant proteins after IUGR [17]. In line with this developmental deregulation, Joss-Moore et al. recently suggested a pivotal role of ECM components such as elastic fibers in the pathomechanism of IUGR-associated lung disease [11]. Although several studies have investigated the synthesis of pulmonary ECM and impaired lung function associated with IUGR, the molecular mechanism linking perturbed ECM with IUGR remains largely unclear to date. Interestingly, human and animal studies demonstrate a programming of inflammatory response subsequent to IUGR [18, 19]. In line with these observations, Plank et al. highlighted a predisposition of former IUGR animals for renal fibrosis and inflammation with a strikingly upregulation of inflammatory and profibrotic marker [Interleukin-6 (IL-6), tumor necrosis factor α (TNF-α), transforming growth factor β (TGF- β)] and of ECM components (collagen I and collagen IV) [20]. It is intriguing though that pulmonary inflammatory response as a link between perturbed ECM and IUGR has not been addressed so far. However, increased expression of cytokines like Interleukin (IL)-13 [21] as well as deregulation of ECM metabolism [22] are known to be involved in the progression of respiratory diseases such as asthma. Furthermore, recent studies underline the central role of IL-6, transforming growth factor (TGF)β1 and plasminogen activator inhibitor-1 (PAI-1) in the development and progression of dysregulated ECM and fibrosis [23, 24].

In this study, we tested the hypothesis that IUGR (1) impairs lung function in a time dependent manner, (2) deregulates both, the expression of profibrotic markers and formation and remodeling of the ECM, and (3) has an impact on pulmonary inflammatory response.

Methods

Animal procedures

All procedures performed on animals were done in accordance with the German regulations and legal requirements and were approved by the local government authorities (Regierung von Mittelfranken). Adult and neonatal Wistar rats were housed in humidity- and temperature-controlled rooms on a 12:12-h light–dark cycle. IUGR in rats was induced by isocaloric low protein diet (8% versus 17% casein) as previously described [25]. On the first postnatal day (P1) the litters were reduced to six pups per dam. During lactation and subsequent to weaning at P23 the animals were fed standard chow. We only used the male rat offspring for the experiments.

Physiological data of control animals and intrauterine growth restricted animals

Body weight was obtained at different time points: P1, P7, P14, P21, P42, P70 by weighing each animal, and weight gain as fold induction in relation birth weight was calculated. Lung weight was obtained by weighing the entire lung at P1, P21, and P70. In addition, the ratio of lung weight to body weight was obtained. Mothers were weighed during gestation at gestational day (G) 1, G7, G14, G21, and G23 as well as during lactation at postnatal day (P) 1, P7, P14, and P23 (day of weaning). Means±standard error of the mean were calculated.

Measurement of airway responsiveness

At the age of P28 and P70, airway responsiveness was assessed by measuring respiratory system resistance (Res) and respiratory system compliance (C_{dyn}) with direct plethysmography (FinePointe™ RC; Wellington, NC, USA). Rats were deeply anesthetized by intramuscular injection of ketamine 100 mg/kg body weight and midazolam 5 mg/kg body weight, tracheotomised and ventilated. Res and C_{dyn} were measured at baseline, and after stimulation with methacholine, a bronchoconstrictor well established for diagnosis of airway hyperresponsiveness.

Tissue preparation

Following anesthesia with ketamine (100 mg/kg body weight) and midazolam (5 mg/kg body weight), the animals were killed. Neonatal animals were euthanized by decapitation. The right lobe of the lung was removed and immediately snap-frozen in liquid nitrogen. The left lobe was inflated via tracheotomy and pressure-fixed at 20 cm H_2O with 4% (mass/vol) paraformaldehyde. Lungs were submersed in 4% (mass/vol) paraformaldehyde overnight for paraffin embedding and sectioned as described previously [26]. Paraffin sections (1 μm) were mounted on poly-L-lysine-coated glass slides, dewaxed with xylene (3–5 min) and rehydrated in a graduated series of ethanol solutions (100%, 95%, and 70% (vol/vol), and finally PBS).

RNA extraction and real-time PCR

Total RNA was isolated from unfixed lung tissue or cultured cells as previously described [27]. Total RNA was screened for mRNA encoding genes listed in Table 1. Quantitative changes in mRNA expression were assessed by quantitative real-time PCR as described previously [25]. In all samples, the relative amount of specific mRNA was normalized to the ubiquitously expressed glyceraldehyd-3-phosphat-dehydrogenase (GAPDH), β-Actin, as well as porphybilinogen-deaminase gene. Primer pairs and TaqMan probes are listed in Table 1. Oligonucleotides were designed with Primer Express software (PerkinElmer, Foster City, CA, USA).

Western blot analysis

Protein extraction, gel electrophoresis and immunoblotting were performed as previously described [26]. Blots were probed with the following antibodies: monoclonal mouse-anti-rat-proliferating cell nuclear antigen (PCNA; DAKO, Glostrup, Denmark, Clone PC10, M0879, 1:10,000), polyclonal rabbit-anti-rat-phospho Stat3 (Cell Signaling, # 9131, 1:1,000), and monoclonal rabbit-anti-rat-Stat3 (Cell Signaling, # 9139, 1:1,000). Monoclonal mouse-anti-rat-β-Actin (Cell Signaling, MA, # 3700, 1:1,000) served as a loading control. Anti-mouse IgG, HRP-linked (Cell Signaling, # 7076, 1:2,000), and HRP-linked anti-rabbit IgG (Cell Signaling, # 7074, 1:2,000) were used as secondary antibodies.

Histology and immunostaining

Tissue preparation was performed as described previously [27]. Sections were incubated with the rabbit-anti-rat collagen I (1:100; Biogenesis, UK). Immune complexes were visualized with an avidin/biotin-DAB (3,3-diamineobenzidine) detection system (Vector Lab, Burlingame, CA, USA). Each slide was counterstained with hematoxylin.

Gelatin zymography

Lung homogenates were incubated with non-denaturating sample buffer (62.5 mM Tris–HCl pH 6.8, 10% glycerol, 2% SDS, 0.0025% bromphenol blue) for 10 min at 37°C and then loaded onto 10% SDS-polyacrylamide gels containing 0.1% gelatin. Following gel electrophoresis, SDS was removed by washing the gel once for 30 min in renaturation buffer (2.5% Tx-100) and once more for 30 min in developing buffer (50 mM Tris–HCl pH 8, 0.2 M NaCl, 5 mM $CaCl_2$, 0.02% Brij 35). Developing of the gel was performed over night at 37°C in developing buffer. For staining of the gel we used 0.1% Coomassie brilliant blue in 25% isopropanol and 10% acetic acid. Imaging was performed with the Biodoc analyze system (Biometra), and densitometry of white bands was measured using the ImageJ software (NIH).

Analysis of data

The results of real-time PCR were calculated based on the ΔΔCt method and expressed as fold induction of mRNA expression compared to the corresponding control group (1.0-fold induction). Densitometric measurement was performed and values were normalized to β-actin. Quantitative evaluation of the immunohistochemical results was performed with the MetaVue™ Imaging System. The Collagen I positive area in a defined area (3.2 mm^2) is displayed in percent. Results are shown as means±standard error of the mean. Two-tailed Mann–Whitney test and two-way ANOVA followed by a Bonferroni post-test were used to assess the significance of differences between IUGR and control animals at given time points. A p value<0.05 was considered as significant.

Results

Intrauterine growth retardation after low protein diet

To analyze maternal weight gain during gestation and lactation we determined maternal body weight from conception (G1) until weaning (P23; Fig. 1a, b). As expected, maternal weight gain was reduced in low protein diet (LP) dams compared to controls during gestation (Fig. 1a). In contrast, during lactation when both experimental groups of dams received standard chow, no difference in weight gain was detectable (Fig. 1b).

The number of animals per litter between control and IUGR dams was not different (15.3±0.9 pups in NP mothers

Table 1 Designed primer pairs and TaqMan probes used in this study

AP-1	Forward 5′-AAACCTTGAAAGCGCAAAACTC-3′
	Reverse 5′-GTGGTTCATGACTTTCTGTTTAAGCT-3′
	Probe 5′-(FAM)-CTGGCGTCCACGGCCAACATG-(TAMRA)-3′
Collagen Iα	Forward 5′-AGAGCGGAGAGTACTGGATCGA-3′
	Reverse 5′-CTGACCTGTCTCCATGTTGCA-3′
	Probe 5′-(FAM)-CAAGGCTGCAACCTGGATGCCATC-(TAMRA)-3′
GAPDH	Forward 5′-ACGGGAAACCCATCACCAT-3′
	Reverse 5′-CCAGCATCACCCCATTTGA-3′
	Probe 5′-(FAM)-TTCCAGGAGCGAGATCCCGTCAAG-TAMRA)-3′
PAI-1	Forward 5′-TCCGCCATCACCAACATTTT-3′
	Reverse 5′-GTCAGTCATGCCCAGCTTCTC-3′
	Probe 5′-(FAM)-CCGCCTCCTCATCCTGCCTAAGTTCTCT-(TAMRA)-3′
IL-6	Forward 5′-TCCAAACTGGATATAACCAGGAAAT-3′
	Reverse 5′-TTGTCTTTCTTGTTATCTTGTAAGTTGTTCTT-3′
	Probe 5′-(FAM)-AATCTGCTCTGGTCTTCTGGAGTTCGGTTTCTA-(TAMRA)-3′
IL-10	Forward 5′-GAAGCTGAAGACCCTCTGGATACA-3′
	Reverse 5′-CCTTTGTCTTGGAGCTTATTAAAATCA-3′
	Probe 5′-(FAM)-CGCTGTCATCGATTTCTCCCCTGTGA-(TAMRA)-3′
IL-13	Forward 5′-GAGCTGAGCAACATCACACAAGA-3′
	Reverse 5′-TGTCAGGTCCACGCTCCAT-3′
	Probe 5′-(FAM)-CAGAAGACTTCCCTGTGCAACAGCAGC-(TAMRA)-3′
MCP-1	Forward 5′-CCTCCACCACTATGCAGGTCTC-3′
	Reverse 5′-GCACGTGGATGCTACAGGC-3′
	Probe 5′(FAM)-TCACGCTTCTGGGCCTGTTGTTCA-(TAMRA)-3′
OPN	Forward 5′-AAAGTGGCTGAGTTTGGCAG-3′
	Reverse 5′-AAGTGGCTACAGCATCTGAGTGT-3′
	Probe 5′(FAM)-TCAGAGGAGAAGGCGCATTACAGCA-(TAMRA)3′
P21	Forward 5′-TGTCTTGCACTCTGGTGTCTCA-3′
	Reverse 5′-CGCTTGGAGTGATAGAAATCTGTTAG-3′
	Probe 5′(FAM)-CCCCTGAGAGGCCTGAAGACTCCC-(TAMRA)3′
TGFβ-1	Forward 5′-CACCCGCGTGCTAATGGT-3′
	Reverse 5′-GGCACTGCTTCCCGAATG-3′
	Probe 5′(FAM)-ACCGCAACAACGCAATCTATGACA-(TAMRA)3′
TNF-α	Forward 5′-GACCCTCACACTCAGATCATCTTCT-3′
	Reverse 5′-TTGTCTTTGAGATCCATGCCATT-3′
	Probe 5′(FAM)-ACGTCGTAGCAAACCACCAAGCGGA-(TAMRA)3′
Adrenoceptor β1[a]	Forward 5′-ATCGTAGTGGGCAACGTGTTG-3′
	Reverse 5′-GGGACATGATGAAGAGGTTGGT-3′
Adrenoceptor β2[a]	Forward 5′-GGATTGCCTTCCAGGAGCTT-3′
	Reverse 5′-TGTCCTACCGTTGCTGTTGCTA-3′
Collagen III[a]	Forward 5′-GGACCTCCTGGTGCTATTG-3′
	Reverse 5′-GAATCCAGGGATACCAGCTG-3′
Elastin[a]	Forward 5′-GAAAACCCCCGAAGCCCT-3′
	Reverse 5′-CCCCACCTTGATATCCCAGG-3′
Fibrillin I[a]	Forward 5′-TGCTCTGAAAGGACCCAATGT-3′
	Reverse 5′-CGGGACAACAGTATGCGTTATAAC-3′
TIMP-1[a]	Forward 5′-GGATATGTCCACAAGTCCCAG-3′
	Reverse 5′-CAGGGCTCAGATTATGCCAG-3′
TIMP-2[a]	Forward 5′-GGACCTGACAAGGACATCG-3′
	Reverse 5′-GATGCTAAGCGTGTCCCAG-3′

[a]TIMP-1, TIMP-2, elastin, and fibrillin were detected by SYBR Green analysis

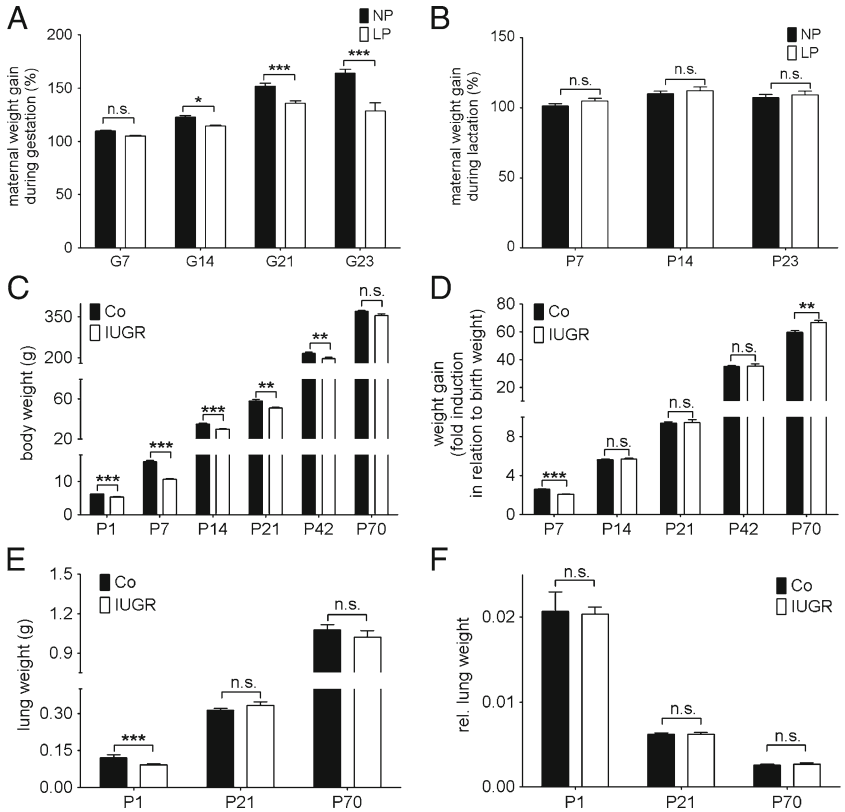

Fig. 1 Body weight, weight gain and lung weight subsequent to IUGR. **a**, **b** Maternal weight gain (%) during gestation (**a**) and during lactation (**b**). Body weight at gestational day (**a**) 1 is 100%, and at postnatal day (P) 1, respectively. n=3–5 mothers per group. Low protein diet during gestation (*LP*; *white bars*) and normal protein diet during gestation (*NP*; control group; *black bars*). **c**, **d** body weight (g) (**c**) and body weight gain (**d**) of rats after IUGR obtained at postnatal day (*P*) 1, P7, P14, P21, P42, and P70. Intrauterine growth restriction (*IUGR*; *white bars*); control animals (*Co*; *black bars*). **e**, **f**: lung weight (**e**) and ratios of lung weight to body weight of rats (**f**) after IUGR at P1, P21, and P70. Intrauterine growth restriction (*IUGR*; *white bars*); control animals (*Co*; *black bars*). n=14–24 (from three to five different litters) for each bar. The significance for each *bar* is indicated by p values, IUGR vs. CO and LP vs. NP. *n.s.* not significant, $^{**}p<0.01$, $^{***}p<0.001$; two-tailed Mann–Whitney test

versus 15.9±0.8 pups in LP mothers, $p>0.05$). At day P1 the average body weight and total lung weight of the undernourished pups (IUGR) was significantly lower than those of age-matched pups of dams fed with normal protein diet (control group; Co; Fig. 1c, e). The IUGR animals remained growth restricted until P42 (Fig. 1c). However, by P70, the IUGR group demonstrated a catch-up growth with an increased weight gain over time (Fig. 1d) and nearly reached the same body mass as the control group (Fig. 1c). In line with this result, the lung also exhibited a notable catch-up growth (Fig. 1e), so that the lung weight between IUGR and control animals did not differ at P70 (Fig. 1e). In addition, we calculated the ratio of lung weight to body weight at P1, P21, and P70 to quantify relative lung weight within the two groups and did not detect any difference at either time point (Fig. 1f). Taken together, low protein diet during gestation led to IUGR and reduced lung weight at birth. Postnatal maternal alimentation with standard chow induced marked catch-up growth of lung and body weight in the offspring until P70.

Effects of IUGR and catch-up growth on the airway responsiveness

Next, we investigated the effect of IUGR on lung function over time, assessed by respiratory airway resistance (Res) and dynamic compliance (C_{dyn}). A marked, but not significant effect of IUGR on both Res and C_{dyn} was already observed at P28 (Fig. 2a, b), where IUGR animals exhibited a slightly increased Res and decreased C_{dyn} compared to the control group (Fig. 2a, b). To further examine whether this altered lung function deteriorates later in adulthood and to demonstrate that this pulmonary impairment is not just ascribable to the differences in body weight at the time of assessment but to the effects of IUGR and postnatal catch-up growth, we assessed Res and C_{dyn} at P70 as well. Strikingly, the Res was significantly increased in IUGR offspring even without methacholine challenge (Fig. 2a). In addition, the C_{dyn} was significantly decreased under baseline conditions subsequent to IUGR at P70 (Fig. 2b). However, C_{dyn} of IUGR animals was unaffected by

inhalation of methacholine, while the control group exhibited decreased C_{dyn} after inhalation of methacholine

Effect of IUGR and catch-up growth on the gene expression of adrenoceptor β1 and β2

To clarify whether altered expression of adrenoceptors as key molecules of the sympathetic nerve system (SNS)—known to regulate bronchoconstriction—might be responsible for the observed differences in airway responsiveness. Therefore, we measured gene expression of both adrenoceptors β1 and β2 by real-time RT-PCR (Fig. 3a, b). Interestingly, no difference was detectable in both genes between IUGR and control group at P1, P42, or P70. Thus, these results give initial evidence, that there is no regulation of adrenoceptors after IUGR.

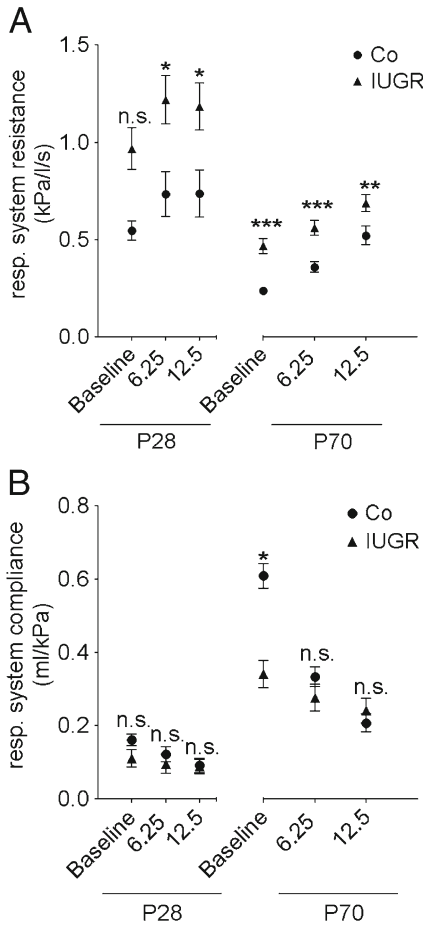

Fig. 2 Effect of IUGR and catch-up growth on respiratory function, assessment of respiratory system resistance (Res) and respiratory system compliance (C_{dyn}) by whole body plethysmography subsequent to intrauterine growth restriction (*IUGR*) at postnatal day 28 (P28) and P70. Res (**a**) and C_{dyn} (**b**) at P28 and P70; baseline (without nebulization), and nebulization of methacholine (two doses, 6.25 mg/ml and 12.5 mg/ml). IUGR (*filled upright triangle*), control (Co; *filled circle*). n=4–17 for each bar (from three to five different litters). The significance for each *bar* is indicated by p values, IUGR vs. CO, *n.s.* not significant; *p<0.05, **p<0.01, ***p<0.001; two-way ANOVA test followed by a Bonferroni post-test (**a**) and two-tailed Mann–Whitney test (**b**)

Effects of IUGR on the production of extracellular matrix components and extracellular matrix metabolizing enzymes in the lung

To address whether the dramatic impairment of lung function is associated with altered composition and production of ECM components, we assessed the expression of genes encoding pivotal ECM molecules over time. Starting at P1, the expression of ECM molecules such as coll III and fibrillin were significantly downregulated, whereas elastin and coll Iα were markedly upregulated, indicating a deregulation of the ECM production (Fig. 4). At P42 and P70, we observed a striking increment of the expression of coll Iα, fibrillin, and elastin (Fig. 4). These results are in line with the quantification of the expression of collagen Iα as a profibrotic marker, assessed by immunostaining at P70 (Fig. 5a). We observed a considerably increased deposition of collagen Iα in the different compartments of the lung (Fig. 5a, b). Next, we investigated ECM turnover assessing the expression of genes encoding the tissue inhibitors of metalloproteinases (TIMP). Interestingly, TIMP-1 and TIMP-2 were markedly upregulated on the mRNA level at P70 (Fig. 5d). Additionally, we analyzed pro-MMP-2—a target of TIMP—by gelatine zymography in total lung homogenate. In line with increased expression of TIMP-1 and TIMP-2, the abundance of pro-MMP-2 was considerably decreased at P70 (Fig. 5e).

In addition, we investigated the expression of genes encoding molecules regulating cell cycle and fibrotic process. Both, p21, a regulator of cell cycle, and AP-1, a profibrotic transcription factor and regulator of differentiation and proliferation, were significantly upregulated at P70 (Fig. 5c).

Taken together, the expression pattern and turnover of ECM components are dynamically regulated in the lung subsequent to IUGR, exhibiting an increased expression, deposition and regulation of ECM molecules at P70 over time with a concomitant increase in expression of regulators of cell cycle and senescence.

Pro-proliferative and pro-senescence state in lungs following IUGR and catch-up growth

To address proliferation and senescence as a feature of fibrotic processes, we assessed the expression of PCNA by immunoblotting. We observed an increasing expression of PCNA in the lungs subsequent to IUGR over time (Fig. 6a, b). To sum up, these results indicate an augmented proliferative state in the mature lung subsequent to IUGR.

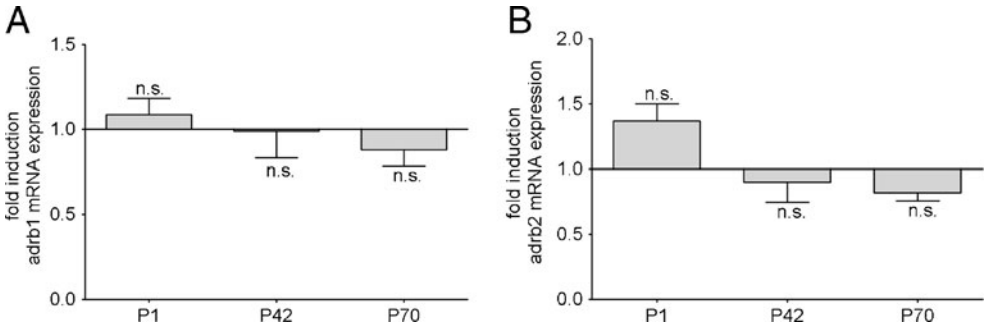

Fig. 3 Effect of IUGR and catch-up growth on the gene expression of adrenoceptor β1 and β2. **a** Expression of adrenoceptor β1 (adrb1) during late lung development and adulthood (P1, P42, and P70). **b**: Expression of adrenoceptor β2 (adrb2) at P1, P42, and P70. The mRNA expression was assessed by quantitative real-time PCR. The control group was normalized to 1; n=6–15 for each group (from three to five different litters). The significance for each *bar* is indicated by p values, IUGR vs. Co; *n.s.* not significant; *$p<0.05$, **$p<0.01$, ***$p<0.001$; two-tailed Mann–Whitney test

Developmental changes in expression of inflammatory cytokines subsequent to IUGR and catch-up growth

To further elucidate the underlying mechanism of impaired lung function, including parenchyma and airways, we assessed the expression of mRNA encoding inflammatory (Fig. 7a) and profibrotic (Fig. 7b) cytokines over time (P1, P42, and P70). We observed a dynamically regulated expression pattern for all analyzed molecules, including Interleukin 6 (IL-6), IL-10, IL-13, tumor necrosis factor alpha (TNF-α), osteopontin (OPN), monocyte chemoattractant protein 1 (MCP-1), plasminogen activator inhibitor (PAI-1), and transforming growth factor beta 1 (TGF-β1; Fig. 7a and b). The expression of inflammatory mediators subsequent to IUGR was decreased at P1, either non altered or considerably increased at P42, and even further increased at P70. Interestingly, the mRNA expression of proinflammatory cytokines was already upregulated at P42 and P70.

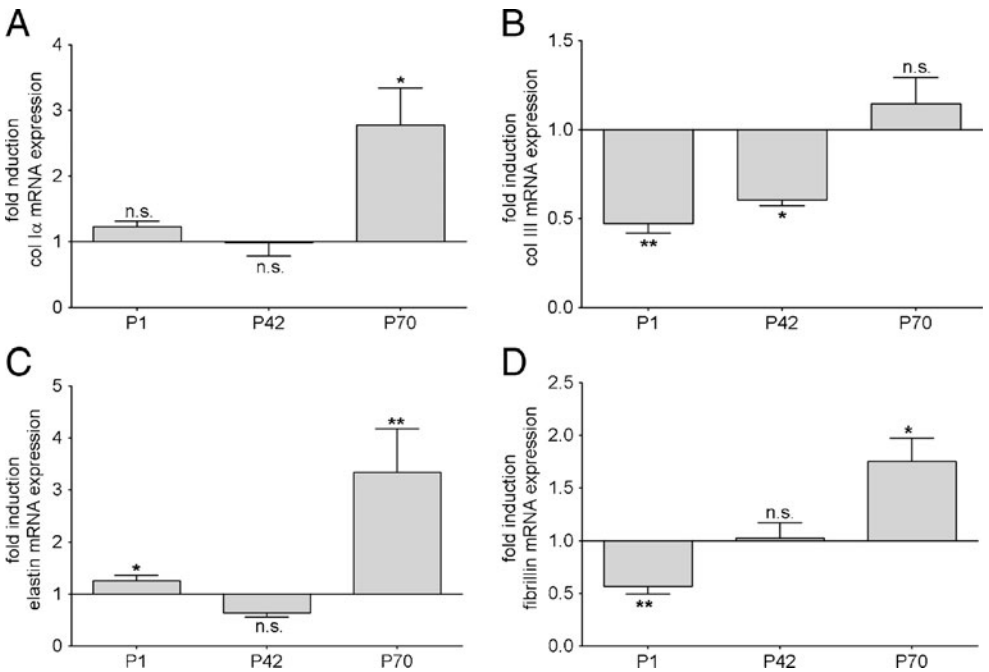

Fig. 4 Effect of IUGR on the expression of extracellular matrix (ECM) proteins and modulators of the ECM. Expression of extracellular matrix (ECM) related genes encoding collagens (Col) Iα (**a**), Col III (**b**), elastin (**c**), and fibrillin (**d**) in lungs extracted at postnatal day 1 (*P1*), P42, and P70 from rats after intrauterine growth restriction (IUGR) and control rats. The mRNA expression, illustrated as relative fold induction, was assessed by real-time PCR. The control group was normalized to 1; n=6–15 for each group (from three to five different litters), *n.s.* not significant; *$p<0.05$, **$p<0.01$; two-tailed Mann–Whitney test

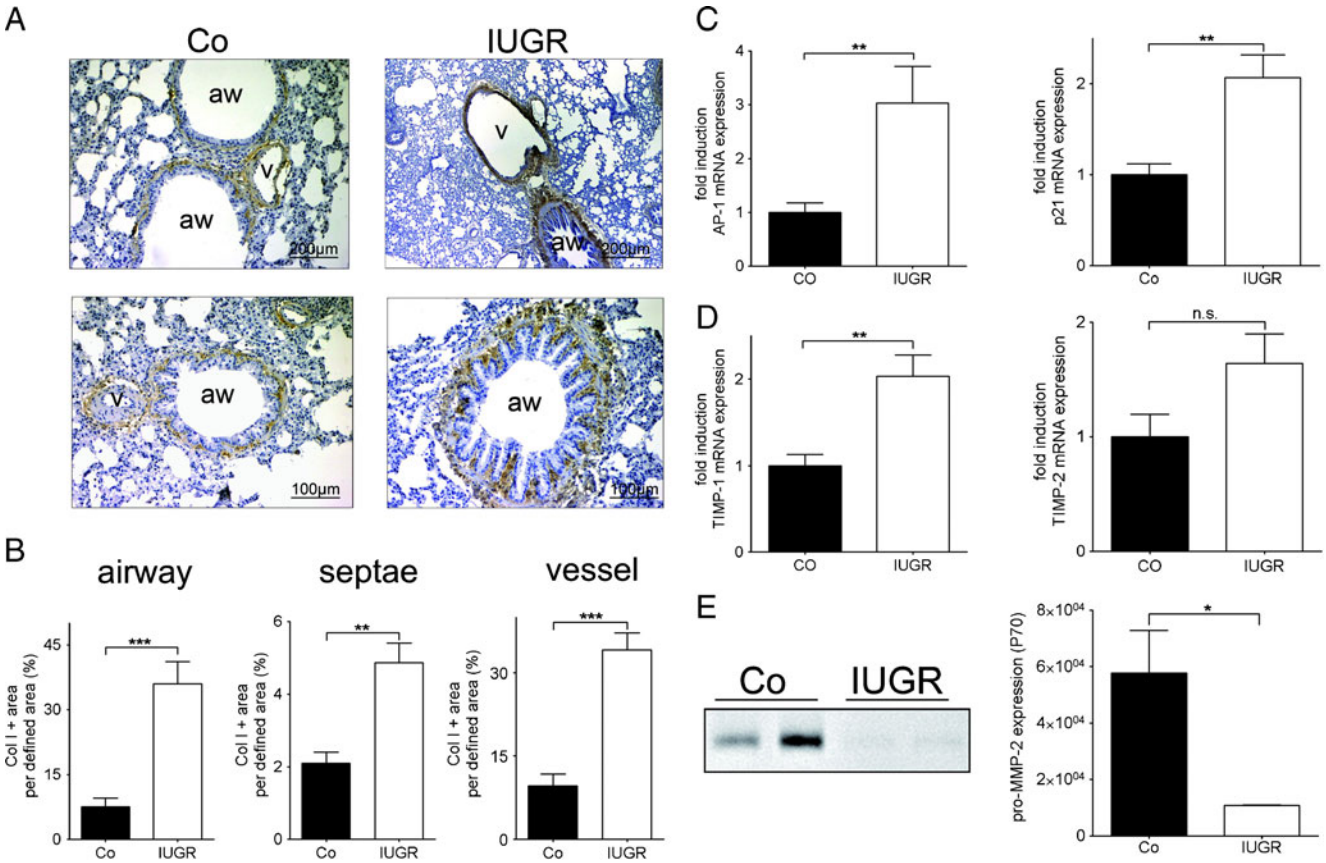

Fig. 5 Effect of IUGR and catch-up growth on ECM composition. **a**, **b** The expression of extracellular matrix (*ECM*) molecule collagen I (*col I*) in the lung was assessed by immunohistochemistry at postnatal day 70 (P70). **a** Representative pictures, illustrating positive col I staining in the alveolar septae, and in perivascular, and peribronchial tissue. **b** Quantitative evaluation of the immunohistochemical results was performed with MetaVue™ Imaging System. *V* vessel, *aw* airway. n=4–6 for each group (from three different litters). **c**, **d** The mRNA expression of genes encoding activator protein 1 (AP-1), p21, tissue inhibitor of metalloproteinases 1 (TIMP-1), and TIMP-2 was assessed by real-time PCR at P70. n=6–12 for each group (from three to five different litters). **e** Analysis of MMP activity in lungs. Representative gelatin zymography of lung tissue at P70 and detection of pro-MMP2 gelatinolytic activity at ~70 kDa (**a**). Quantification pro-MMP-2 activity at P70. n=4–6 for each group. The significance for each *bar* is indicated by p values, IUGR (*white bar*) and control group (*black bar*), *n.s.* not significant; *p<0.05, **p<0.01, ***p<0,001; two-tailed Mann–Whitney test

In contrast, the abundance of IL-10 mRNA, a mediator with anti-inflammatory effects, was decreased at P42 and unchanged at P70 (Fig. 7a). In conclusion, we observed a dynamic regulation of inflammatory mediators in animals subsequent to IUGR, starting with an attenuated inflammatory state at P1, and then an inversion over time to a markedly augmented inflammatory response.

Activation of Stat3 in the lung subsequent to IUGR and catch-up growth

To further elucidate the intracellular signaling of inflammatory cytokines and the activity of these signaling pathways, we assessed the expression and activation of Stat3 by immunoblotting (Fig. 8a and b). Consistent with the elevated expression of IL-6, we detected an increased phosphorylation of Stat3 at P70, whereas the phosphorylation was unchanged at P1 and P42. Furthermore, the target genes of Stat3, such as TIMP-1 and AP-1 were concomitantly increased at P70 (Fig. 5c, d). In conclusion, the activation of the intracellular proinflammatory cascade as represented by Stat3 phosphorylation is markedly increased in lungs at P70 subsequent to IUGR.

Discussion

There is increasing evidence that prenatal factors, such as nutritional supply, permanently influence pivotal processes of lung development and maturation of pulmonary structures [9, 10]. The pathogenic mechanisms that results in an impairment of lung function observed in IUGR-associated lung disease are poorly understood. Although several studies have demonstrated an important role of ECM in lung disease subsequent to IUGR, the impact of pulmonary inflammation as a potential link between IUGR and

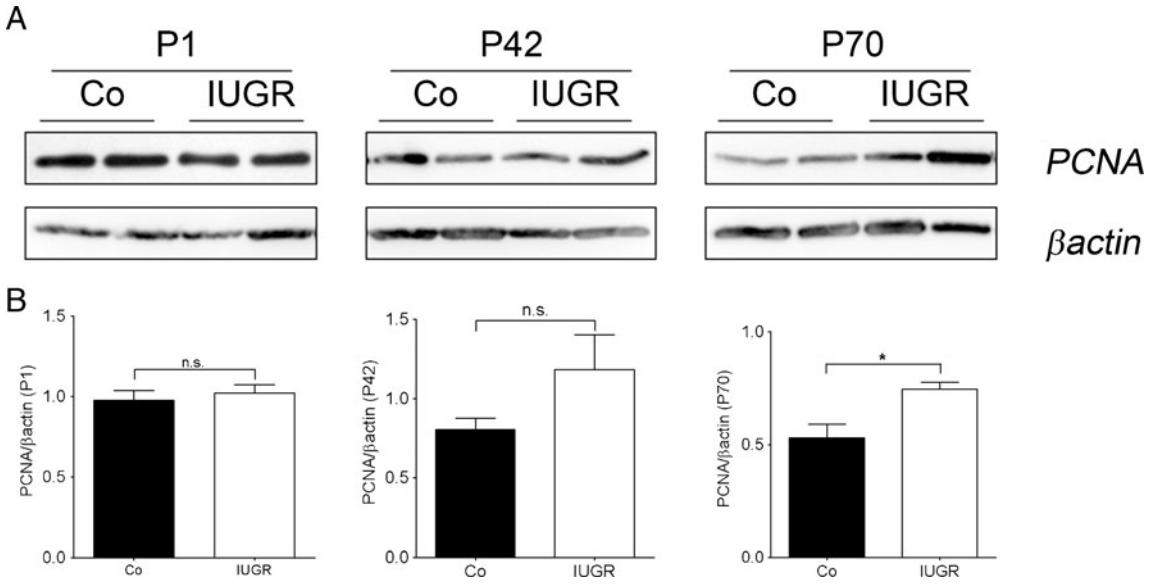

Fig. 6 Effect of IUGR and catch-up growth on proliferation. **a**, **b** Representative immunoblots of proliferating cell nuclear antigen (*PCNA*) (**a**) and the quantification of the expression by densitometric analysis (**b**) at postnatal day 1 (P1), P42, and P70, using constitutively expressed β-actin as loading control. The significance for each *bar* is indicated by *p* values, intrauterine growth restriction (*IUGR*; *white bar*) and control group (*black bar*); *n.s.* not significant; **p*<0.05, ***p*<0.01; two-tailed Mann–Whitney test, *n*=4–6 for each group (from three to five different litters)

pulmonary disease has not been addressed to date. In this study, we aimed to examine the inflammatory processes as well as ECM over time, starting at P1 and terminating at P70.

In line with a report by Joyce et al. [28], our study shows airway hyperresponsiveness following IUGR. Obstructive lung diseases are associated with an enhanced deposition and a deregulated expression of ECM components [21].

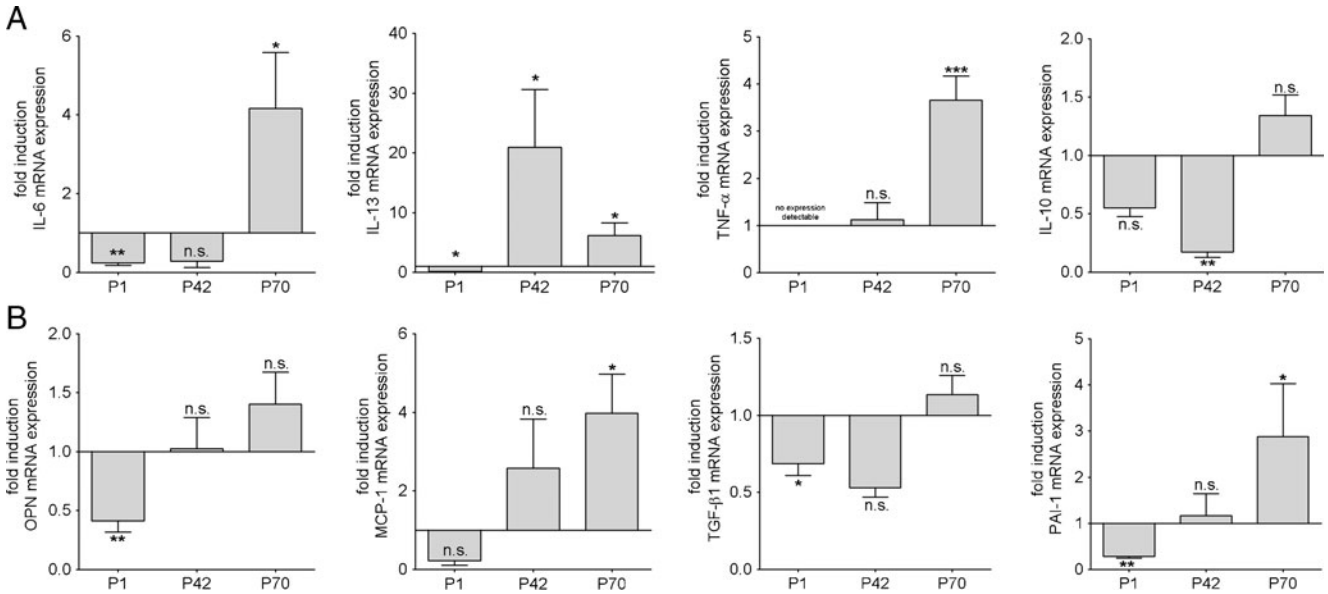

Fig. 7 Effect of IUGR and catch-up growth on the expression of proinflammatory and profibrotic cytokines in the lung. **a** Expression of proinflammatory genes encoding Interleukin-6 (IL-6), IL-13, tumor necrosis alpha (TNF-α), and IL-10 during late lung development and adulthood (P1, P42, and P70). **b** Expression of profibrotic genes encoding osteopontin (OPN), monocyte chemottractant protein 1 (MCP-1), transforming growth factor beta (TGF-β), TGF-β1, and plasminogen activator inhibitor-1 (PAI-1) at P1, P42, and P70. The mRNA expression was assessed by quantitative real-time PCR. The control group was normalized to 1; *n*=6–15 for each group (from three to five different litters). The significance for each *bar* is indicated by *p* values, IUGR vs. Co; *n.s.* not significant; **p*<0.05, ***p*<0.01, ****p*<0.001; two-tailed Mann–Whitney test

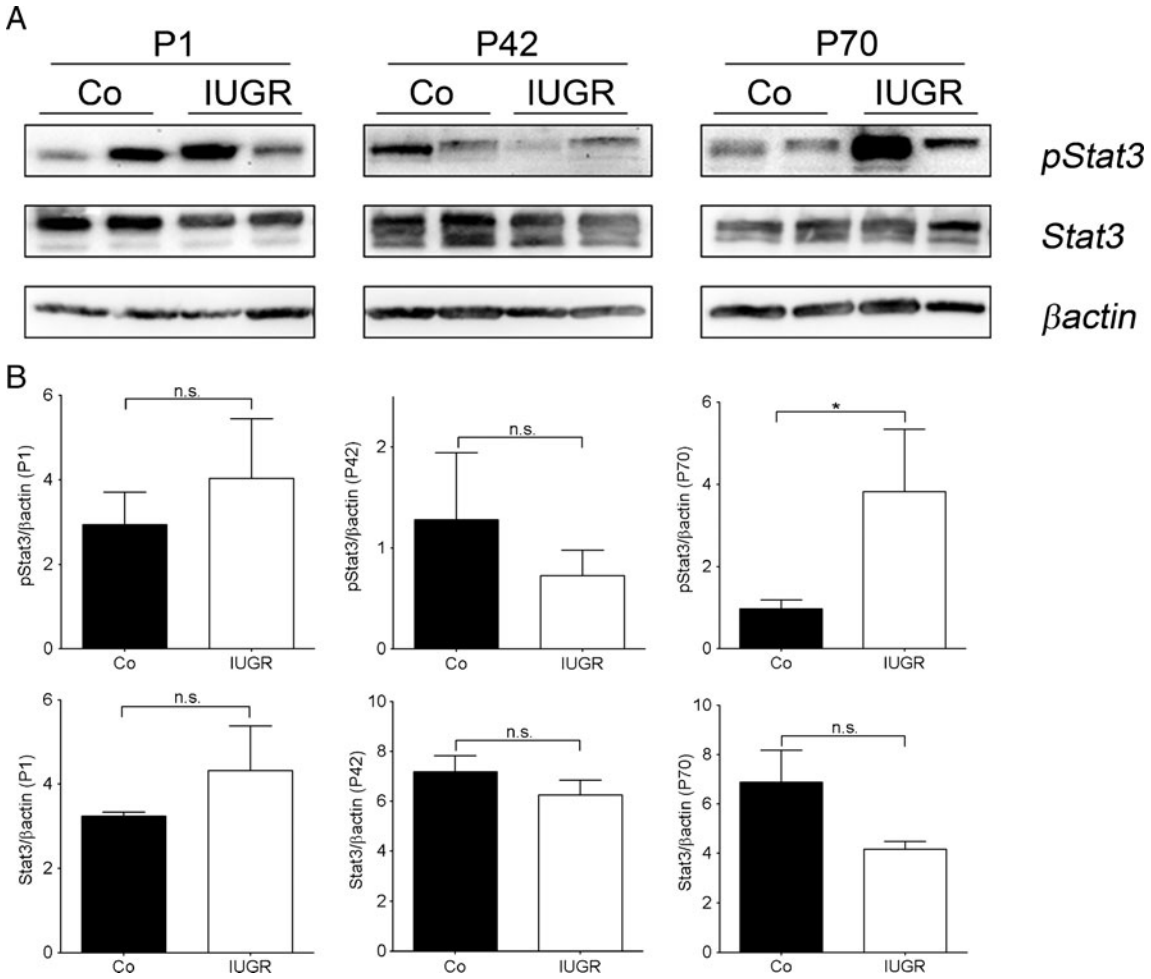

Fig. 8 Stat3 signaling in lungs subsequent to IUGR and catch-up growth. **a** Representative immunoblots, illustrating the expression and phosphorylation of Signal transducer and activator of transcription 3 (*Stat3*) in lungs subsequent to intrauterine growth restriction (*IUGR*) at postnatal day (P1), P42, and P70. Expression and phosphorylation of Stat3 was assessed by immunoblot, using constitutively expressed β-Actin as loading control. **b** Quantification of the expression and phosphorylation of Stat3 by densitometric analysis, using β-Actin as loading control. The significance for each *bar* is indicated by *p* values, IUGR (*white bars*) vs. CO (*black bars*), *n.s.* not significant; **p*<0.05, ***p*<0.01; two-tailed Mann–Whitney test, *n*=4–6 for each group (from three to five different litters)

Pulmonary structure and ECM have been previously investigated and demonstrated to be affected by intrauterine growth restriction. How are the ECM components regulated over time subsequent to IUGR? Experimental studies revealed a dysregulated lung development [7] and alterations of lung structure [8] in adult animals subsequent to IUGR induced by placental insufficiency. Similarly, a very recent study of our group demonstrated that rats following IUGR exhibit an increased mean linear intercept (MLI) at P70, while septal thickness remains unaffected, indicating an elevated amount of alveolar tissue [15]. In line with these morphometric results, analysis of key enzymes regulating apoptotic processes revealed a dampened apoptosis at P1. Thus, consistent with the given dampened apoptosis during late lung development [15], and the significantly increased proliferative state shown in the present study, data we describe in both studies give a strong body of evidence that the balance between apoptosis and proliferation is perturbed and proliferation is favored the more development and age proceed. Furthermore, the results in the present study demonstrate a decreased production of ECM at P1 (collagen III and fibrillin) and an increasing deposition of ECM molecules, such as collagen Iα and fibrillin at P70. Even more interesting than the dynamic regulation of the gene expression of ECM components is the evidence of an augmented deposition of collagen Iα in the different compartments of the lung at P70, indicating profibrotic processes. Experimental studies of Maritz et al. [8, 29] support these profibrotic processes shown in this study giving evidence of a persistently thicker blood–air barrier and thicker septa. In accordance with dysregulated lung morphology, we demonstrated the reduced MLI in a previous study. Here, we show a deregulation of ECM deposition, finally leading to loss of function and thereby to impaired lung function. However, possibly, the profibrotic

processes in our animal model with catch-up growth are in an initial state and therefore P70 is too early for the animals to exhibit a thickening of the septal wall. Later time points will be essential to get a broader understanding of the dynamics and the consequences of the deregulated ECM.

The ECM is deposited by fibroblasts and is continuously remodeled by matrix remodeling proteases. MMP-2 and TIMP-2 are strongly expressed in rodents during lung development [30] and in fibrotic processes [31], indicating a pivotal role and finely tuned regulation of matrix remodeling in the lung. In our study, we have illustrated that IUGR markedly decreased the protein expression of pro-MMP-2 at P70. Interestingly, this deregulation was accompanied by a significantly increased expression of the inhibitors of metalloproteinases, TIMP-1 and TIMP-2, and an augmented deposition of collagen Iα in the lung. In conclusion, our data collectively suggest that IUGR would swing the balance in favor of interstitial ECM deposition and would prevent turnover of ECM components in the lung. In addition, we demonstrate an elevation of p21 at P70. Several studies report the impact of p21 on the regulation of cell cycle and cell aging/senescence, by inhibiting the activity of cyclin-dependent kinases [32]. Regulation of p21 expression is mediated by various pathways, such as Stat-signaling [33], activated by inflammatory cytokines.

It is intriguing that inflammatory response over time and pulmonary inflammation as a potential pathomechanism for impaired regulation of tissue remodeling and subsequent fibrosis in IUGR animals has not been addressed to date. First, we chose to quantify mRNA expression of several genes encoding cytokines known to have an important impact on inflammatory processes. Strikingly, this study clearly reveals a continuously increasing expression of inflammatory cytokines, such as IL-6, IL-13 and PAI-1, starting being markedly decreased at P1 and significantly upregulated at later time points (P42 and P70). These findings are in line with studies demonstrating a predisposition for fibrosis and inflammation in other organs subsequent to IUGR [20] and the notable role of IL-6 in the pathomechanism of fibrosis [34]. For example, Plank et al. illustrated the devastating course of thy1-glomerulophritis in IUGR-rats with clear features of renal inflammation and fibrosis [25]. Consistent with these results, the renal expression of IL-6, PAI-1, and MCP-1 was dramatically upregulated and the kidneys displayed an increased deposition of ECM in a rat model of glomerulonephritis following IUGR [25]. However, inflammatory cytokines, such as IL-6, are not just crucial for inflammatory processes but also for normal lung development. Interestingly, we demonstrated a significant downregulation of IL-6 at the transition from saccular to alveolar phase at P1. The diminished abundance of IL-6 at this crucial stage of late lung development may contribute to the deregulation of lung morphogenesis. The evidence that IL-6 mediates the catch-up growth of hypoplastic lungs [35] demonstrates its impact on lung development and underlines our idea. At P42 and P70, however, the picture is reversed: the expression of IL-6, IL-13, PAI-1, and TNF-α is significantly increased. Airway overexpression of IL-6 contributes to subepithelial fibrosis with collagen deposition [36]. The elevated expression of IL-6 could be a link to the observed catch-up growth in animals subsequent to IUGR in our model. Zhu and colleagues [37] showed in mice that an overexpression of IL-13 in the lungs causes an asthmatic phenotype with mononuclear inflammation, subepithelial fibrosis, and airway obstruction. Furthermore, Hattori and colleagues [38] demonstrated that PAI-1-deficient mice are protected from bleomycin-induced pulmonary fibrosis. PAI-1 and the plasminogen system play an important role in airway remodeling by inhibiting MMP and therefore preventing degradation of ECM as it is seen in asthmatic lung diseases [39]. To highlight the incremental inflammatory response induced by IUGR, we analyzed the intracellular signaling of several cytokines, focusing on the Stat3 pathway and its target genes, such as TIMP-1 and AP-1. The decision to focus on Stat3 signaling was based two crucial findings in our group: first, previous studies of Plank et al. demonstrated in an experimental model of glomerulonephritis that IUGR aggravates the course of the disease and led to fibroproliferative processes, impairment of renal function and increased inflammatory response. Interleukin-6 (IL-6) was the cytokine with the most striking increment in gene expression [25]. Interestingly, this cytokine is also elevated in the present study. Furthermore, the downstream pathway of IL-6 is Stat3-mediated. Second, very recent experiments from our group focusing on renal endocrine function subsequent to catch-up growth show also a strong increment in IL-6 gene expression. In accordance with these findings investigation of Stat3 signaling in the present study demonstrates a significant deregulation. Strikingly, we detected an augmentation in phosphorylation over time, starting with no changes at P1 and terminating with a significant increment on phosphorylation compared to the control group at P70. The fact that the increment of inflammatory response is paralleled by elevated expression and deposition of ECM components is especially interesting and leads to the assumption that inflammation may be a potential underlying mechanism of the profibrotic pulmonary processes. Furthermore, this study demonstrates that pulmonary impairment subsequent to IUGR is accompanied by postnatal catch-up growth. This may represent an additional pathogenetic factor for the impairment of the lung seen in our animals. However, that cannot be completely clarified in our study and require further experiments.

The impact and the underlying mechanisms of increased inflammatory response in IUGR-associated lung disease remains poorly understood. Epigenetics is one of the key

mechanisms widely discussed and increasingly recognized in the broad field of developmental programming. Several studies demonstrated persistent changes in methylation of promoter regions of crucial developmental genes following fetal and postnatal programming, ultimately leading to physiological dysfunction [40–43]. In the present study, expression of numerous cytokines is increased in lungs after IUGR. Before addressing epigenetics, it will thus be crucial to identify the key player in mediating the observed inflammatory response. Intensive research is encouraged to delineate the underlying mechanism and to find treatment strategies to improve or even prevent lung diseases caused by IUGR. It will be promising to determine the effect of an anti-inflammatory therapy on the development of IUGR-associated lung diseases in further studies in order to address the question whether such treatment strategies may help to prevent the onset of pulmonary damage and improve long term lung function following IUGR.

Taken together, the present results demonstrate that IUGR impairs lung function, leads to a dynamic upregulation of inflammatory signaling and subsequently to a profibrotic remodeling of ECM over time. Thus, this study does not only contribute to a better general understanding of pathological consequences in the increasingly important clinical group of IUGR infants, but also elucidates the pathomechanistic aspects of IUGR-associated lung disease. This will ultimately allow defining more effective preventive and therapeutic strategies of pulmonary disease.

Acknowledgments The authors thank Ida Allabauer and Julia Dobner for expert technical assistance and Andrea Hartner (Department of Pediatric and Adolescent Medicine, University Hospital Erlangen, Germany) for access to microscopy facilities. The animal experiments were in part supported by a grant to Jörg Dötsch, Christian Plank, and Wolfgang Rascher by the Deutsche Forschungsgemeinschaft, Bonn, Germany; SFB 423, Collaborative Research Centre of the German Research Foundation: Kidney Injury: Pathogenesis and Regenerative Mechanisms, Project B13 and by a grant to Christian Plank and Miguel Angel Alejandre Alcázar by the Erlanger Leistungsbezogene Anschubfinanzierung und Nachwuchsförderung (ELAN) Erlangen, Köln Fortune, University of Cologne.

Disclosure The authors declare no conflict of interest.

References

1. Meetoo D (2008) Chronic diseases: the silent global epidemic. Br J Nurs 17:1320–1325
2. Ljustina-Pribic R, Petrovic S, Tomic J (2010) Childhood asthma and risk factors. Med Pregl 63:516–521
3. Bloomberg GR (2011) The influence of environment, as represented by diet and air pollution, upon incidence and prevalence of wheezing illnesses in young children. Curr Opin Allergy Clin Immunol 11:144–149. doi:10.1097/ACI.0b013e3283445950
4. Gilliland FD, Li YF, Peters JM (2001) Effects of maternal smoking during pregnancy and environmental tobacco smoke on asthma and wheezing in children. Am J Respir Crit Care Med 163:429–436
5. Barker DJ (1995) Intrauterine programming of adult disease. Mol Med Today 1:418–423
6. Nuyt AM (2008) Mechanisms underlying developmental programming of elevated blood pressure and vascular dysfunction: evidence from human studies and experimental animal models. Clin Sci (Lond) 114:1–17. doi:10.1042/CS20070113
7. Lipsett J, Tamblyn M, Madigan K, Roberts P, Cool JC, Runciman SI, McMillen IC, Robinson J, Owens JA (2006) Restricted fetal growth and lung development: a morphometric analysis of pulmonary structure. Pediatr Pulmonol 41:1138–1145
8. Maritz GS, Cock ML, Louey S, Suzuki K, Harding R (2004) Fetal growth restriction has long-term effects on postnatal lung structure in sheep. Pediatr Res 55:287–295. doi:10.1203/01.PDR.0000106314.99930.65
9. Maritz GS, Morley CJ, Harding R (2005) Early developmental origins of impaired lung structure and function. Early Hum Dev 81:763–771. doi:10.1016/j.earlhumdev.2005.07.002
10. Kotecha SJ, Watkins WJ, Heron J, Henderson J, Dunstan FD, Kotecha S (2010) Spirometric lung function in school-age children: effect of intrauterine growth retardation and catch-up growth. Am J Respir Crit Care Med 181:969–974. doi:10.1164/rccm.200906-0897OC
11. Joss-Moore LA, Wang Y, Yu X, Campbell MS, Callaway CW, McKnight RA, Wint A, Dahl MJ, Dull RO, Albertine KH et al (2011) IUGR decreases elastin mRNA expression in the developing rat lung and alters elastin content and lung compliance in the mature rat lung. Physiol Genomics 43:499–505. doi:10.1152/physiolgenomics.00183.2010
12. Warburton D, Bellusci S (2004) The molecular genetics of lung morphogenesis and injury repair. Paediatr Respir Rev 5:S283–287
13. Copland I, Post M (2004) Lung development and fetal lung growth. Paediatr Respir Rev 5:S259–264
14. Orgeig S, Crittenden TA, Marchant C, McMillen IC, Morrison JL (2010) Intrauterine growth restriction delays surfactant protein maturation in the sheep fetus. Am J Physiol Lung Cell Mol Physiol 298:L575–583. doi:10.1152/ajplung.00226.2009
15. Alejandre Alcazar MA, Morty RE, Lendzian L, Vohlen C, Oestreicher I, Plank C, Schneider H, Dotsch J (2011) Inhibition of TGF-beta signaling and decreased apoptosis in IUGR-associated lung disease in rats. PLoS One 6:e26371. doi:10.1371/journal.pone.0026371
16. Cock ML, Albuquerque CA, Joyce BJ, Hooper SB, Harding R (2001) Effects of intrauterine growth restriction on lung liquid dynamics and lung development in fetal sheep. Am J Obstet Gynecol 184:209–216. doi:10.1067/mob.2001.108858
17. Gagnon R, Langridge J, Inchley K, Murotsuki J, Possmayer F (1999) Changes in surfactant-associated protein mRNA profile in growth-restricted fetal sheep. Am J Physiol 276:L459–465
18. Amarilyo G, Oren A, Mimouni FB, Ochshorn Y, Deutsch V, Mandel D (2011) Increased cord serum inflammatory markers in small-for-gestational-age neonates. J Perinatol 31:30–32. doi:10.1038/jp.2010.53
19. Desai M, Gayle DA, Casillas E, Boles J, Ross MG (2009) Early undernutrition attenuates the inflammatory response in adult rat offspring. J Matern Fetal Neonatal Med 22:571–575. doi:10.1080/14767050902874105
20. Plank C, Nusken KD, Menendez-Castro C, Hartner A, Ostreicher I, Amann K, Baumann P, Peters H, Rascher W, Dotsch J (2010) Intrauterine growth restriction following ligation of the uterine arteries leads to more severe glomerulosclerosis after mesangioproliferative glomerulonephritis in the offspring. Am J Nephrol 32:287–295. doi:10.1159/000319045
21. Wynn TA (2003) IL-13 effector functions. Annu Rev Immunol 21:425–456. doi:10.1146/annurev.immunol.21.120601.141142

22. Gueders MM, Foidart JM, Noel A, Cataldo DD (2006) Matrix metalloproteinases (MMPs) and tissue inhibitors of MMPs in the respiratory tract: potential implications in asthma and other lung diseases. Eur J Pharmacol 533:133–144. doi:10.1016/j.ejphar.2005.12.082
23. Pedroza M, Schneider DJ, Karmouty-Quintana H, Coote J, Shaw S, Corrigan R, Molina JG, Alcorn JL, Galas D, Gelinas R et al (2011) Interleukin-6 contributes to inflammation and remodeling in a model of adenosine mediated lung injury. PLoS One 6:e22667. doi:10.1371/journal.pone.0022667
24. Wygrecka M, Jablonska E, Guenther A, Preissner KT, Markart P (2008) Current view on alveolar coagulation and fibrinolysis in acute inflammatory and chronic interstitial lung diseases. Thromb Haemost 99:494–501. doi:10.1160/TH07-11-0666
25. Plank C, Ostreicher I, Hartner A, Marek I, Struwe FG, Amann K, Hilgers KF, Rascher W, Dotsch J (2006) Intrauterine growth retardation aggravates the course of acute mesangioproliferative glomerulonephritis in the rat. Kidney Int 70:1974–1982. doi:10.1038/sj.ki.5001966
26. Alejandre-Alcazar MA, Kwapiszewska G, Reiss I, Amarie OV, Marsh LM, Sevilla-Perez J, Wygrecka M, Eul B, Kobrich S, Hesse M et al (2007) Hyperoxia modulates TGF-beta/BMP signaling in a mouse model of bronchopulmonary dysplasia. Am J Physiol Lung Cell Mol Physiol 292:L537–549. doi:10.1152/ajplung.00050.2006
27. Alejandre Alcazar MA, Boehler E, Amann K, Klaffenbach D, Hartner A, Allabauer I, Wagner L, von Horsten S, Plank C, Dotsch J (2011) Persistent changes within the intrinsic kidney-associated NPY system and tubular function by litter size reduction. Nephrol Dial Transplant 26:2453–2465. doi:10.1093/ndt/gfq825
28. Joyce BJ, Louey S, Davey MG, Cock ML, Hooper SB, Harding R (2001) Compromised respiratory function in postnatal lambs after placental insufficiency and intrauterine growth restriction. Pediatr Res 50:641–649
29. Maritz GS, Cock ML, Louey S, Joyce BJ, Albuquerque CA, Harding R (2001) Effects of fetal growth restriction on lung development before and after birth: a morphometric analysis. Pediatr Pulmonol 32:201–210. doi:10.1002/ppul.1109
30. Ryu J, Vicencio AG, Yeager ME, Kashgarian M, Haddad GG, Eickelberg O (2005) Differential expression of matrix metalloproteinases and their inhibitors in human and mouse lung development. Thromb Haemost 94:175–183. doi:10.1267/THRO05010175
31. Oggionni T, Morbini P, Inghilleri S, Palladini G, Tozzi R, Vitulo P, Fenoglio C, Perlini S, Pozzi E (2006) Time course of matrix metalloproteases and tissue inhibitors in bleomycin-induced pulmonary fibrosis. Eur J Histochem 50:317–325
32. Sherr CJ, Roberts JM (1995) Inhibitors of mammalian G1 cyclin-dependent kinases. Genes Dev 9:1149–1163
33. Chin YE, Kitagawa M, Su WC, You ZH, Iwamoto Y, Fu XY (1996) Cell growth arrest and induction of cyclin-dependent kinase inhibitor p21 WAF1/CIP1 mediated by STAT1. Science 272:719–722
34. Saito-Fujita T, Iwakawa M, Nakamura E, Nakawatari M, Fujita H, Moritake T, Imai T (2011) Attenuated lung fibrosis in interleukin 6 knock-out mice after C-ion irradiation to lung. J Radiat Res (Tokyo) 52:270–277
35. Nogueira-Silva C, Moura RS, Esteves N, Gonzaga S, Correia-Pinto J (2008) Intrinsic catch-up growth of hypoplastic fetal lungs is mediated by interleukin-6. Pediatr Pulmonol 43:680–689. doi:10.1002/ppul.20840
36. Gharaee-Kermani M, Phan SH (2005) Molecular mechanisms of and possible treatment strategies for idiopathic pulmonary fibrosis. Curr Pharm Des 11:3943–3971
37. Zhu Z, Homer RJ, Wang Z, Chen Q, Geba GP, Wang J, Zhang Y, Elias JA (1999) Pulmonary expression of interleukin-13 causes inflammation, mucus hypersecretion, subepithelial fibrosis, physiologic abnormalities, and eotaxin production. J Clin Invest 103:779–788. doi:10.1172/JCI5909
38. Hattori N, Mizuno S, Yoshida Y, Chin K, Mishima M, Sisson TH, Simon RH, Nakamura T, Miyake M (2004) The plasminogen activation system reduces fibrosis in the lung by a hepatocyte growth factor-dependent mechanism. Am J Pathol 164:1091–1098. doi:10.1016/S0002-9440(10)63196-3
39. Kucharewicz I, Kowal K, Buczko W, Bodzenta-Lukaszyk A (2003) The plasmin system in airway remodeling. Thromb Res 112:1–7. doi:10.1016/j.thromres.2003.10.011
40. Simmons RA (2007) Role of metabolic programming in the pathogenesis of beta-cell failure in postnatal life. Rev Endocr Metab Disord 8:95–104. doi:10.1007/s11154-007-9045-1
41. Pinney SE, Simmons RA (2010) Epigenetic mechanisms in the development of type 2 diabetes. Trends Endocrinol Metab 21:223–229. doi:10.1016/j.tem.2009.10.002
42. Plagemann A, Harder T, Brunn M, Harder A, Roepke K, Wittrock-Staar M, Ziska T, Schellong K, Rodekamp E, Melchior K et al (2009) Hypothalamic proopiomelanocortin promoter methylation becomes altered by early overfeeding: an epigenetic model of obesity and the metabolic syndrome. J Physiol 587:4963–4976. doi:10.1113/jphysiol.2009.176156
43. Plagemann A, Roepke K, Harder T, Brunn M, Harder A, Wittrock-Staar M, Ziska T, Schellong K, Rodekamp E, Melchior K et al (2010) Epigenetic malprogramming of the insulin receptor promoter due to developmental overfeeding. J Perinat Med 38:393–400. doi:10.1515/JPM.2010.051